

# Heat Transfer Characteristics of 3d Flow of $\gamma Al_2O_3 - C_2H_6O_2$ and $Al_2O_3 - H_2O$ Nanofluids Over a Rotating Disk Subject to Newtonian Heating

Majid Amin\*, Muhammad Asim Ullah†, Izaz Ali‡

## Abstract

*In this paper, the main focus is to study Heat transfer characteristics of 3D flow of and Nanofluids over a rotating disk subject to Newtonian heating to improve the thermal conductivity and stability of different systems in engineering and science field. This type of Newtonian play vital in industrial field. The experimental values improve the thermal conductivity process. The main objectives our work is to obtain the graphical result and numerical result to show the efficiency of the nanofluids. The governing equations of the proposed model are highly nonlinear due to which the exact solution is difficult, sometimes impossible, the numerical solution is suitable to find the solution of such a model. A mathematical analysis is eventually provided to prove why the nanofluids are advantageous as far as the heat transfer enhancement is concerned. Firstly, using transformation, the system is converted into a dimensionless form and then converted to first order systems and then solved using the RK4 scheme. The present research performs a greater role in industrial and biological fields. These types of nanofluid are very attractive areas for researchers and scientists. The thermal efficiency of these types of nanofluid performs a good work in food stuff problems and enhances the engine efficiency for a long period of life. The outcome of different constraints on temperature and velocity distribution is displayed graphically.*

**Keywords:** Nano-fluid, RK4 Method, Newtonian fluid, Dimensionless Parameter, Nonlinear Differential Equations.

## Introduction

In an ordinary state all the fluids do not offer good thermal conductivity. This gap is fulfilled through Nano-fluids which is actually the addition of solid particles which are very small in size called nanoparticles and base liquids. Commonly used nanoparticles are graphene, carbon nanotubes, carbides and oxides and general base fluids are water, engine oil and ethylene glycol.

A fluid is sometimes used in a device to prevent overheating and the body will remain cool. The high thermal conductivity and high

---

\*Qurtuba University of Science and Information Technology Peshawar, k-1, Phase 3, Hayatabad, Peshawar, Pakistan, [enr.maamin55@gmail.com](mailto:enr.maamin55@gmail.com)

† Qurtuba University of Science and Information Technology Peshawar, k-1, Phase 3, Hayatabad, Peshawar, Pakistan, [asimkhanicp@gmail.com](mailto:asimkhanicp@gmail.com)

‡Faculty of Mechanical Engineering University of Ljubljana, Askerceva 6, 1000 Ljubljana, Slovenia, [izazaliutk@gmail.com](mailto:izazaliutk@gmail.com)

stability of the nanofluid put some well-known properties of the nanofluids. High heat with holding capacity, enhanced heat transfer properties, minimum viscosity, cheap cost, friendly environment that is not polluting the atmosphere and efficient cooling system. Nanofluids play a very important role in information technology and automobile industries, efficient cooling in nuclear radiators.

Most applications of nanofluids flow study by spinning disk are in the machine rotation, chemical industries and engineering, thermal power generation systems, medical apparatus, phenomena of crystal growing, electronic and computer storage devices, air purification machines, Turbo machinery and so on. Mustafa in (Mustafa Turkyilmazoglu, 2016) studied the movement of viscous fluids through a rotating disk. Effects of specified type of temperature in a viscous fluid transmission have been studied by Turkyilmazoglu and Senel (M Turkyilmazoglu & Senel, 2013) over a permeable spinning geometry. in (Mustafa Turkyilmazoglu, 2014)examine the MHD fluid over a spinning disk.

A nanofluid flow mass transmission in viscous fluid flow has been studied by Turkyilmazoglu and Senel (M Turkyilmazoglu & Senel, 2013)over a permeable spinning disk. Mustafa (Rashidi, Kavyani, & Abelman, 2014) examined the MHD flow over a spinning disk. A Nano-fluid flow and its applications on a rotating disk are presented by Turkyilmazoglu (Hatami, Sheikholeslami, & Ganji, 2014). Analysis of nanofluids flow through spinning and contracting disk, reported by (Sheikholeslami, Hatami, & Ganji, 2015). During fluid motion, they analyzed the effect of the embedded parameters. Sheikholeslami et al. (Sheikholeslami et al., 2015) studied the Nano-liquid flow over an inclined rotating disk. They examined the thermal and cooling efficiency of the Nano-fluid.

It is the characteristics of fluid that it has no fixed shape. It means that its shape can change easily due to external pressure. In a fluid the intermolecular forces between the molecules is very weak due to this behavior, it moves or adopt the shape of a container (Mukhopadhyay & Nimbalkar, 2021). This is true without the fluid we can't survive because without water or blood how the life is possible. Water is a main source of life due to which it is used in most things. Now a day it is mixed with nanoparticles, which enhance the efficiency of the engine. Those kinds of fluids which satisfy Newton's law of viscosity are known as Newtonian fluid(Mahadevappa, 1980). Newton's law states that "Shear stress is directly related to the gradient of velocity". i.e.  $\tau \propto \frac{du}{dy}$  .

Alumina ( $Al_2O_3$ ) is usually used for Nano size particles to make better thermal conductivity of nano-liquids  $Al_2O_3$  nano-liquid has attracted the attention of researchers in some freezing processes (Maré, Sow, Halelfadl, Lebourlout, & Nguyen, 2012). According to their size  $Al_2O_3$  very small size particles are divided into 2 kinds  $\alpha Al_2O_3$  and  $\gamma Al_2O_3$ . Maciver et al. (Maciver, Tobin, & Barth, 1963) examined the properties of the modules problem, specific type of eta and gamma alumina. The spray scattering process on the stretched exterior part of the cylinder with nanometer sized of  $Al_2O_3$  and  $Cuo$  water based Nano-fluid has been studied by Alshomrani and Gul (Alshomrani & Gul, 2017), considering the influence of a number of different flow parameter systems by applying the optimal controlling scheme. In a closed system, Nguyen et al. (Nguyen, Roy, Gauthier, & Galanis, 2007) experimentally examined the properties, heat transfer rate of  $Al_2O_3$  water base nano-liquid flow. In diesel generators, Kulkarni et al. (Kulkarni, Vajjha, Das, & Oliva, 2008) used  $Al_2O_3$  nano-liquid as a coolant to increase the specific heat performance. Forced convective flow, Zamzamian et al. (Zamzamian, Oskouie, Doosthoseini, Joneidi, & Pazouki, 2011) comprehensively discussed the irregular flow of the nano-liquid of  $Al_2O_3 - C_2H_6O_2$  and  $CuO - C_2H_6O_2$ .

On the inside of a square crack, Sebdani et al. (Sebdani, Mahmoodi, & Hashemi, 2012) considered the mixed convection flow under the influence of heat, motion of the nano-liquid of  $Al_2O_3 - H_2O$ . The definite type of  $\gamma Al_2O_3 - H_2O$  and  $\gamma Al_2O_3 - C_2H_6O_2$  nano-liquid is elaborated by Rashidi et al. (Rashidi, Vishnu Ganesh, Abdul Hakeem, Ganga, & Lorenzini, 2016) using the model of Prandtl number, they numerically solved the velocity and temperature model and inspected the nano-liquid flow on the upright side of the flexible sheet. They investigated graphically the impact of different flow parameters of nano-liquid of  $\gamma Al_2O_3 - H_2O$  and  $\gamma Al_2O_3 - C_2H_6O_2$  on the velocity and the temperature profile. In addition, the consequence parameters of engineering interest, skin friction and rate of the heat conversation (Nu) is contained in this effort and the same study to squeeze the flow effort is achieved using both numerical and analytical methods among the parallel plates  $\gamma Al_2O_3 - H_2O$ . And  $\gamma Al_2O_3 - C_2H_6O_2$  nano-liquid is described in (Ahmed, Adnan, Khan, & Mohyud-Din, 2017), (Ahmed, Adnan, Khan, & Mohyud-Din, 2018). Nusselt number (Nu) is a dimensionless number defined as “The rate of heat transfer of convection divide by conduction at a boundary in a fluid”(Thomas & Casasayas, 2022).

The outcome of Nusselt number and skin friction for each  $\gamma Al_2O_3 - H_2O$  and  $\gamma Al_2O_3 - C_2H_6O_2$  nano-liquid is highlighted by graphical analysis. During the examination, they observed that  $\gamma Al_2O_3 - C_2H_6O_2$  nano-liquid is the dominant role as  $\gamma Al_2O_3 - H_2O$  nano-liquid. Numerically three dimensional flows are  $\gamma Al_2O_3 - H_2O$  and  $\gamma Al_2O_3 - C_2H_6O_2$  nano-liquids among the parallel rotating plates have been investigated by Khan et al. (U. Khan, Adnan, Ahmed, & Mohyud-Din, 2017). In water and different organic solvents, stable dispersion of the Aluminum oxide, especially (Ethylene Glycol). Its main purpose is to use these Nano-fluids for heat engines rotating disks which are used in various industrial applications and solar cells etc.

The mathematical modeling of the rotating disk and its implementation of the industry is the key point of this research. In fact, modeling and simulation plays a dynamic role in the field of material sciences and engineering. It keeps an investigational test balanced and sometimes very valuable to identify those physical results that cannot be identified experimentally. The similar work related to nanofluids using different geometries can be seen in (Gul, Afridi, Ali, Khan, & Alshomrani, 2018)(N. S. Khan, Gul, Islam, Khan, & Shah, 2017)(Tahir et al., 2017)(W. Khan, Gul, Idrees, Islam, & Khan, 2017). In the field of engineering, researchers usually encounter strong nonlinear boundary value problems that can't be solved exactly. In view of a non-linear character of the models, various numerical techniques are adopted to find the solution. The Runge –Kutta numerical scheme (W. Khan et al., 2017)(Umar, Adnan, Naveed, & Tauseef, 2012) is frequently used for the solution of nonlinear ODEs.

This scheme is very strong, convergent and responsive to the common computers. The detailed stepwise approach of this method has been discussed. A careful review of the literature shows that the 3D rotating  $\gamma Al_2O_3 - H_2O$  and  $\gamma Al_2O_3 - C_2H_6O_2$  Nano-fluids flow on rotating disk was not reported by thermal convection and its solution through RK4. It's noticed that no one has studied three dimensional nanofluid flows under the impact of the operative Prandtl model over a rotating disk. The present work performs a vital role in the field of science and engineering. The mentioned nanofluid enhances the thermal efficiency, which is used in nuclear cooling reactors, food stuff problem, and cancer therapy. Hopefully based on the present work a good research can be performed in future. In section 2, a brief discussion for the proposed research process is presented. In Section 3 and 4 applications of this method and numerical results are considered and graphically

presented for the proposed scheme. Section 5 ends this paper with a brief conclusion.

### Mathematical Modeling

The three dimensional nano-liquid flows are considered over an extending and spinning disk. The mathematical phenomena for the nano-liquids motion is settled in such a manner that the disk turns with an angular velocity  $\omega$  at  $z=0$ . Two dissimilar kinds of Nano-fluid  $\gamma Al_2O_3 - H_2O$  and  $\gamma Al_2O_3 - C_2H_6O_2$  are considered from experimental results. Due to axial symmetry of the disk, the derivatives of  $\theta$  are neglected. The surface temperature is represented by  $T_f$  while the ambient fluid temperature is  $T_\infty$  and the velocity components are presented by  $(u, v, w)$ .

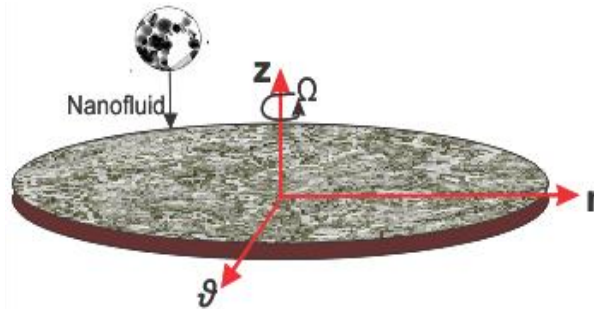


Figure 2.1: Geometry of the problem

Basic equations of the flow problem are expressed as [9]:

$$\frac{\partial}{\partial r}(ru) + \frac{\partial}{\partial z}(rw) = 0,$$

(1)

$$\rho_{nf} \left[ u \frac{\partial u}{\partial r} - \frac{v^2}{r} + w \frac{\partial u}{\partial z} \right] = \mu_{nf} \left[ \frac{\partial^2 u}{\partial r^2} + \frac{1}{r} \left( \frac{\partial u}{\partial r} \right) - \frac{u}{r^2} + \frac{\partial^2 u}{\partial z^2} \right], \quad (2)$$

$$\rho_{nf} \left[ u \left( \frac{\partial v}{\partial r} \right) + \frac{uv}{r} + w \left( \frac{\partial v}{\partial z} \right) \right] = \mu_{nf} \left[ \frac{\partial^2 v}{\partial r^2} + \frac{1}{r} \left( \frac{\partial v}{\partial r} \right) + -\frac{v}{r^2} + \frac{\partial^2 v}{\partial z^2} \right], \quad (3)$$

$$\rho_{nf} \left[ u \left( \frac{\partial w}{\partial r} \right) + w \left( \frac{\partial w}{\partial z} \right) \right] = \mu_{nf} \left[ \frac{\partial^2 w}{\partial r^2} + \frac{1}{r} \left( \frac{\partial w}{\partial r} \right) + \frac{\partial^2 w}{\partial z^2} \right], \quad (4)$$

$$(\rho c_p)_{nf} \left[ u \frac{\partial T}{\partial r} + w \frac{\partial T}{\partial z} \right] = k_{nf} \left[ \frac{\partial^2 T}{\partial r^2} + \frac{1}{r} \left( \frac{\partial T}{\partial r} \right) + \frac{\partial^2 T}{\partial z^2} \right]. \quad (5)$$

Specified boundary conditions related to problem are discussed (Tahir et al., 2017):

$$u = rs, \quad v = r\omega, \quad w = 0, \quad -k_{nf} \frac{\partial T}{\partial z} = h_f (T_f - T) \quad \text{at } z = 0, \quad (6)$$

$$u \rightarrow 0, \quad v \rightarrow 0, \quad T \rightarrow T_\infty \quad \text{at } z \rightarrow \infty.$$

Now  $u, v, w$  are the velocity components in the radial, azimuthal and axial directions  $(r, \theta, z)$  and  $T$  (local temperature),  $\rho_{nf}$  (specific density),  $(\rho c_p)_{nf}$  (specific heat capacity),  $k_{nf}$  (Thermal conductivity),  $\mu_{nf}$  (dynamic viscosity) of nanofluids. Furthermore, we have used the effective Prandtl model (Rashidi et al., 2016)(Ahmed et al., 2017)(Ahmed et al., 2018) for this problem.

The physical properties of the nanoparticles from the experimental approach have been defined as:

$$\rho_{nf} = \left\{ (1 - \phi) + \left( \frac{\rho_s}{\rho_f} \right) \phi \right\} \rho_f, \quad (7)$$

$$(\rho c_p)_{nf} = \left\{ (1 - \phi) + \left( \frac{(\rho c_p)_s}{(\rho c_p)_f} \right) \phi \right\} (\rho c_p)_f.$$

The  $\phi$  here represent the volume fraction of the nanofluids. For  $\gamma Al_2O_3 - H_2O$  aluminum oxide base water nanofluid (Rashidi et al., 2016)(Ahmed et al., 2017)(Ahmed et al., 2018), the experimental values of Pr,  $\mu_{nf}$ , and  $k_{nf}$  are defined as:

$$\mu_{nf} = 123.0\phi^2 \mu_f + 7.30\phi \mu_f + 1.0\mu_f, \quad (8)$$

$$k_{nf} = 4.970\phi^2 k_f + 2.720\phi k_f + 1.0k_f, \quad (9)$$

$$Pr_{nf} = 82.10\phi^2 Pr_f + 3.90\phi Pr_f + 1.0Pr_f. \quad (10)$$

For  $\gamma Al_2O_3 - C_2H_6O_2$  (Nano sized alumina, ethylene glycol) (Rashidi et al., 2016)(Ahmed et al., 2017). Experimental values of  $Pr$ ,  $\mu_{nf}$  and  $k_{nf}$  are defined as:

$$\mu_{nf} = 306.0\phi^2 \mu_f - 0.190\phi \mu_f + 1.0\mu_f, \quad (11)$$

$$k_{nf} = 28.9050\phi^2 k_f + 2.82730\phi k_f + 1.0k_f, \quad (12)$$

$$Pr_{nf} = 254.30\phi^2 Pr_f + 3.000\phi Pr_f + 1.0Pr_f. \quad (13)$$

The specific fixed attachment of physical quantities is described by equations (7-13) which are  $\rho_f$ ,  $\mu_f$ ,  $k_f$  and  $(\rho c_p)_f$ . Also  $\rho_f$ ,  $\mu_f$ ,  $k_f$  and  $(\rho c_p)_f$  shows specific density, dynamic viscosity, thermal conductivity and specific heat of the base fluids, whereas  $\rho_s$ ,  $\mu_s$  is the specific density, dynamic viscosity of solid nanoparticles and the suitable similarity transformation is defined as follows:

$$u = r\omega \frac{df(\eta)}{d\eta}, \quad v = r\omega g(\eta), \quad w = -\sqrt{2\nu_f \omega} f(\eta), \quad \Theta(\eta) = \frac{T - T_\infty}{T_f - T_\infty}, \quad \eta = z \sqrt{\frac{2\omega}{\nu_f}}. \quad (14)$$

(Alshomrani & Gul, 2017)

Subsequently, by using the relationship and the similarity quantities in equations (6-13) for Nano-fluid model  $\gamma Al_2O_3 - C_2H_6O_2$  and  $\gamma Al_2O_3 - H_2O$ . The Eq.(1.1) is automatically satisfied and the Eqs.(2-6) have been transformed to the set of nonlinear ODEs. A non-dimensional system succeeding set of ODEs, show the steady flow of  $\gamma Al_2O_3 - C_2H_6O_2$  and  $\gamma Al_2O_3 - H_2O$  nanofluid, which we get over the rotating disc. The momentum boundary layer in Eqs (2-4) and the thermal boundary layers in Eq. (5) are transformed for  $\gamma Al_2O_3 - H_2O$ . Nano-fluid as:

$$\frac{d^3}{d\eta^3} f(\eta) + (123.0\phi^2 + 7.30\phi + 1.0) \left( (1 - \phi) + \phi \frac{\rho_s}{\rho_f} \right) \left( f(\eta) \frac{d^2 f(\eta)}{d\eta^2} - \frac{1}{2} \left( \frac{df(\eta)}{d\eta} \right)^2 \right) + \frac{1}{2} (g(\eta))^2 = 0 \quad (15)$$

$$\frac{d^2g(\eta)}{d\eta^2} + (123\phi^2 + 7.3\phi + 1) \left( (1-\phi) + \phi \frac{\rho_s}{\rho_f} \right) \left( f(\eta) \frac{dg(\eta)}{d\eta} - \frac{df(\eta)}{d\eta} g(\eta) \right) = 0, \quad (16)$$

$$\frac{(4.97\phi^2 + 2.72\phi + 1)}{Pr_f(82.1\phi^2 - 3.9\phi + 1)} \frac{d^2\Theta(\eta)}{d\eta^2} + \left( (1-\phi) + \phi \frac{(\rho C_p)_s}{(\rho C_p)_f} \right) f(\eta) \frac{d\Theta(\eta)}{d\eta} = 0. \quad (17)$$

The momentum boundary layer in Eqs. (2-4) and the thermal boundary layer in Eq.(5) are transformed for  $\gamma Al_2O_3 - C_2H_6O_2$  nanofluid as:

$$\frac{d^3}{d\eta^3} f(\eta) + (306.0\phi^2 - 0.190\phi + 1.0) \left( (1-\phi) + \phi \frac{\rho_s}{\rho_f} \right) \left( f(\eta) \frac{d^2f(\eta)}{d\eta^2} - \frac{1}{2} \left( \frac{df(\eta)}{d\eta} \right)^2 + \frac{1}{2} (g(\eta))^2 \right) = 0, \quad (18)$$

$$\frac{d^2g(\eta)}{d\eta^2} + (306\phi^2 - 0.19\phi + 1) \left( (1-\phi) + \phi \frac{\rho_s}{\rho_f} \right) \left( f(\eta) \frac{dg(\eta)}{d\eta} - \frac{df(\eta)}{d\eta} g(\eta) \right) = 0, \quad (19)$$

$$\frac{(28.905\phi^2 + 2.8273\phi + 1)}{Pr_f(254.3\phi^2 - 3.00\phi + 1)} \frac{d^2\Theta(\eta)}{d\eta^2} + \left( (1-\phi) + \phi \frac{(\rho C_p)_s}{(\rho C_p)_f} \right) f(\eta) \frac{d\Theta(\eta)}{d\eta} = 0. \quad (20)$$

The physical conditions for the momentum boundary layer (2-4) and thermal boundary layer Eq. (5). Presented in Eq. (6) which is transformed into the equation below:

$$f(0) = 0, \frac{d}{d\eta} f(0) = C, g(0) = 0, \frac{d}{d\eta} \Theta(0) = -\frac{k_f Bi}{k_{nf}}, \quad (21)$$

$$\frac{d}{d\eta} f(\infty) \rightarrow 0, g(\infty) \rightarrow 0, \Theta(\infty) \rightarrow 0.$$

The non-dimensional parameters archived from the governing equations after using the transformation in Eq. (14) are defined as:

$$C = \frac{s}{\omega}, Pr = \frac{(\mu C_p)_f}{k_f}, Bi = \frac{h_f}{k_f} \sqrt{\frac{\nu_f}{2\omega}}. \quad (22)$$

Here  $C$  stands for the stretching-strength parameter,  $Pr$  stand for Prandtl number, the name of Prandtl number was first given by German physicist Ludwing Prandtl. It is defined as “The division of *The Sciencetech* **124** **Volume 4, Issue 2, April-June 2023**



momentum diffusivity by thermal diffusivity” (Moatimid, Hassan, & Mohamed, 2020)

$$\text{Pr} = \frac{\nu}{\alpha} = \frac{\mu C_p}{k}.$$

*Bi* Stand for the Biot number Biot number was first introduced by French physicist Jean Biot. It is a dimensionless quantity used for calculation of heat transfer. It is defined as “the resistance of heat transfers inside the body divided by heat transfer at the surface of the body (GANDI, 2016)”. Mathematically, we can write as:

$$\text{Bi} = \frac{Lh}{k}.$$

The two terms rate of heat transfer and the Skin friction coefficient are defined as:

$$R_{e_r}^{\frac{1}{2}} C_f = \left( \left( \frac{d^2 f(0)}{d\eta^2} \right)^2 + \left( \frac{dg(0)}{d\eta} \right)^2 \right)^{\frac{1}{2}}, \quad R_{e_r}^{-\frac{1}{2}} Nu = -\frac{k_{nf}}{k_f} \left( \frac{d\Theta(0)}{d\eta} \right). \quad (23)$$

Here  $R_{e_r} = \frac{2\omega r^2}{\nu_f}$  stand for the local Reynolds number.

### Solution strategy

The exact solution of the coupled and nonlinear flow model is unlikely. Therefore, the approximate or numerical method is required to handle these problems. The current thermal flow model has been tackled through a famous numerical method known as Runge-Kutta numerical technique (Ahmed et al., 2017) (Ahmed et al., 2018) (U. Khan et al., 2017) (Gul et al., 2018) (N. S. Khan et al., 2017). At the beginning, the system of higher order differential equations will be converted into a set of first order initial value problems.

The modeled equation (15-17) for  $\gamma Al_2O_3 - H_2O$  nano-fluid and equations (18-20) for the  $\gamma Al_2O_3 - C_2H_6O_2$  nanofluid with boundary conditions in equation (21) are transformed into first order system using the mention variables as:

$$y_1 = f(\eta), y_2 = \frac{df(\eta)}{d\eta}, y_3 = \frac{d^2 f(\eta)}{d\eta^2}, y_4 = g(\eta), y_5 = \frac{dg(\eta)}{d\eta}, y_6 = \Theta(\eta), y_7 = \frac{d\Theta(\eta)}{d\eta}. \quad (24)$$

The numerical RK4 method has been implemented to the first order ODEs system (15-17) with the efforts of the proposed variables given in Eq. (24). The first order ODEs system for the  $\gamma Al_2O_3 - H_2O$

Nano-fluid has been obtained in Equation (25). The first orders ODEs system for the  $\gamma Al_2O_3 - C_2H_6O_2$  nanofluid has been obtained as equation (26). And the initial conditions are settled as Equation (27).

$$\begin{aligned} \frac{dy_1}{d\eta} &= y_2, \\ \frac{dy_2}{d\eta} &= y_3, \\ \frac{dy_3}{d\eta} &= -(123\phi^2 + 7.3\phi + 1) \left( (1-\phi) + \phi \frac{\rho_s}{\rho_f} \right) \left[ y_1 y_3 - \frac{1}{2} y_2^2 + \frac{1}{2} y_4^2 \right], \\ \frac{dy_4}{d\eta} &= y_5, \\ \frac{dy_5}{d\eta} &= -(123\phi^2 + 7.3\phi + 1) \left( (1-\phi) + \phi \frac{\rho_s}{\rho_f} \right) [y_1 y_5 - y_2 y_4], \\ \frac{dy_6}{d\eta} &= y_7, \\ \frac{dy_7}{d\eta} &= -\frac{\text{Pr}_f (82.1\phi^2 + 3.9\phi + 1)}{(4.97\phi^2 + 2.72\phi + 1)} \left( (1-\phi) + \phi \frac{(\rho C_p)_s}{(\rho C_p)_f} \right) (y_1 y_7). \end{aligned} \quad (25)$$

$$\begin{aligned} \frac{dy_1}{d\eta} &= y_2, \\ \frac{dy_2}{d\eta} &= y_3, \\ \frac{dy_3}{d\eta} &= -(306\phi^2 - 0.1\phi + 1) \left( (1-\phi) + \phi \frac{\rho_s}{\rho_f} \right) \left[ y_1 y_2 - \frac{1}{2} y_2^2 + \frac{1}{2} y_4^2 \right], \\ \frac{dy_4}{d\eta} &= y_5, \\ \frac{dy_5}{d\eta} &= -(306\phi^2 - 0.1\phi + 1) \left( (1-\phi) + \phi \frac{\rho_s}{\rho_f} \right) [y_1 y_5 - y_2 y_4] \end{aligned}$$

$$\frac{dy_6}{d\eta} = y_7,$$

$$\frac{dy_7}{d\eta} = -\frac{Pr_f(254.3\phi^2 - 3.0\phi + 1)}{28.905\phi^2 + 2.8273\phi + 1} \left( (1 - \phi) + \phi \frac{(\rho C_p)_s}{(\rho C_p)_f} \right) (y_1 y_7) \quad (26)$$

$$y_1 = 0, \quad y_2 = C, \quad y_3 = u_1, \quad y_4 = 0, \quad y_5 = u_2, \quad y_6 = -\frac{k_f Bi}{k_{nf}}, \quad y_7 = u_3. \quad (27)$$

**Table 3.1**

Indicate the experimental values of thermal properties of Ethyle-water and Alumina (Rashidi et al., 2016)(Ahmed et al., 2017) Physical properties

(Pr)  $c_p$  (J / kgK)  $k$  (W / m) K  $\rho$  (kg / m<sup>3</sup>)

Alumina (Al <sub>2</sub> O <sub>3</sub> )		765	40	3970
Pure water (H <sub>2</sub> O)		6.964182	0.6099	8.3
Ethylene glycol (C <sub>2</sub> H <sub>6</sub> O <sub>2</sub> )		2042384	0.249	1116.6

**Table 3.2**

Displays the effect of  $\phi$  versus  $-f''(0)$  (skin friction) and  $-g'(0)$  (Nusselt number) for the nanofluid  $\gamma Al_2O_3 - H_2O$ .

$\phi$	$-f''(0)$	$-g'(0)$	$-\Theta'(0)$
0.1	3.6329	5.6983	6.4311
.2	5.7226	9.0006	4.8772
0.3	7.9498	12.5195	3.7556
0.4	10.2217	16.1171	2.9481

**Table 3.3**

Displays the effect of  $\phi$  versus  $-f''(0)$  (skin friction) and  $-g'(0)$  (Nusselt number) for the nanofluid  $\gamma Al_2O_3 - C_2H_6O_2$ .

$\phi$	$-f''(0)$	$-g'(0)$	$-\Theta'(0)$
0.1	4.2390	6.6580	5.4079
0.2	7.6498	12.0450	3.1231
0.3	11.2270	17.7116	1.9103

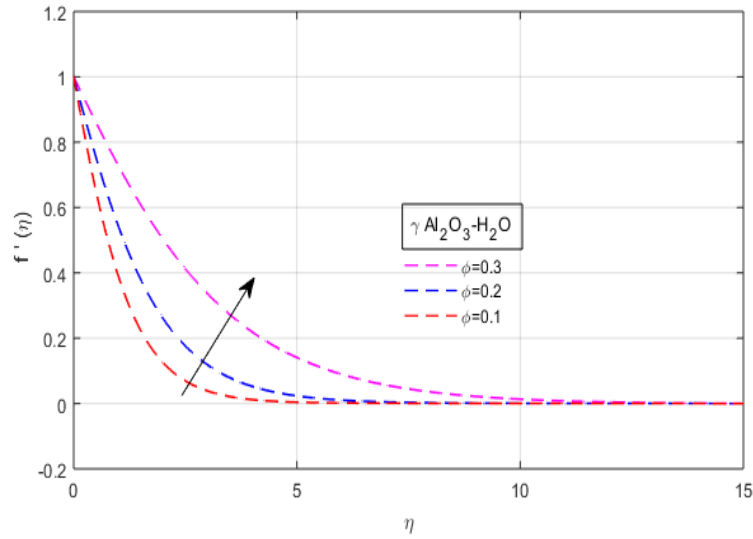


Figure 3.1: Impact of  $\phi$  versus  $\gamma\text{Al}_2\text{O}_3 - \text{H}_2\text{O}$  Nano-fluid. Where  $\text{Pr} = 6.4, B_i = 8.5, C = 1$ .

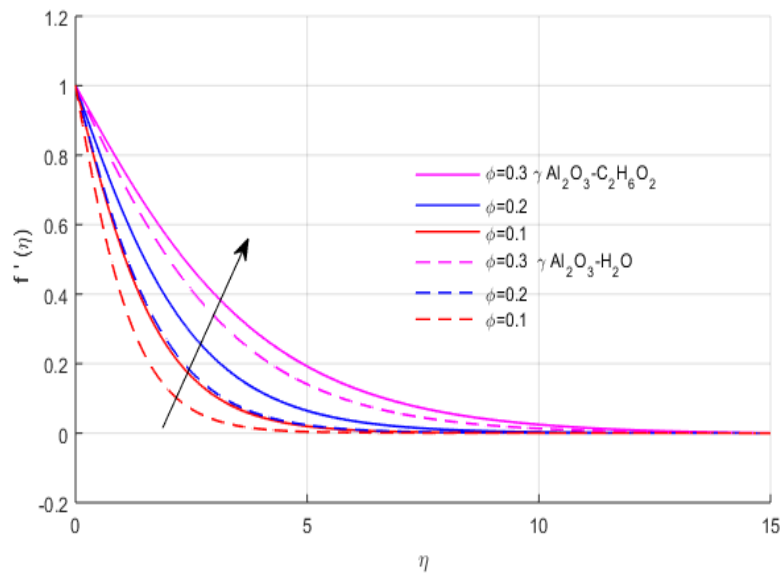


Figure3.3: Variation in  $\frac{df(n)}{dn}$  for various values of  $\phi$ . When  $Pr = 6.4, B_i = 8.5, C = 1$ .

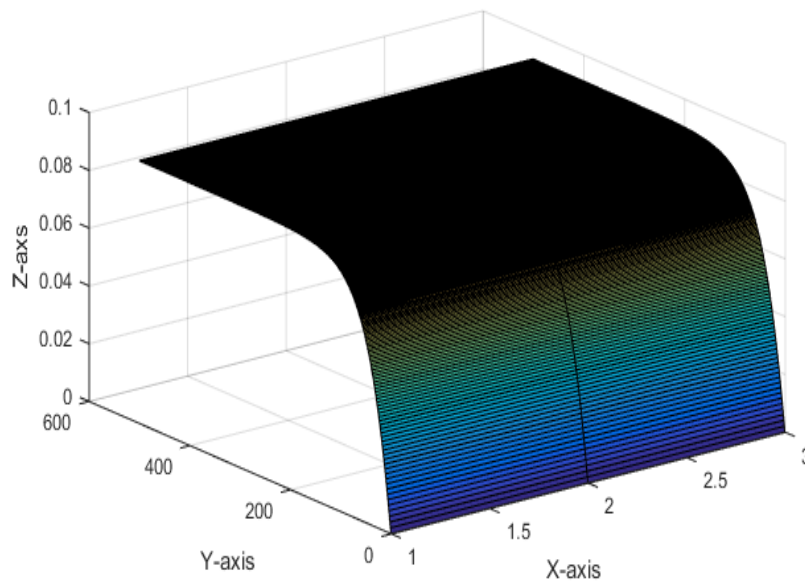


Figure 3.4: Variation in  $f(\eta)$  for various values of  $\phi$ . When  $Pr = 6.4, B_i = 8.5, C = 1$ .

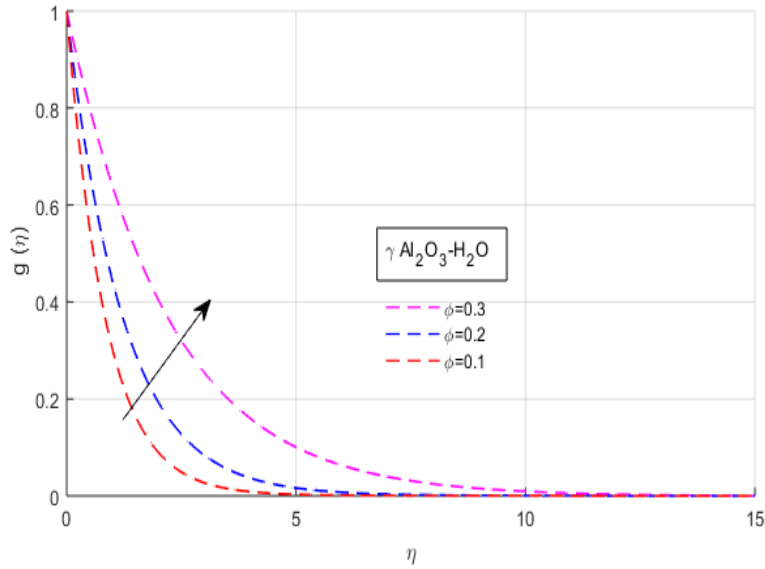


Figure 3.5: Variation in  $g(\eta)$  versus  $\phi$ , When  $Pr = 6.4, B_i = 8.5, C = 1$ , for the  $\gamma\text{Al}_2\text{O}_3 - \text{H}_2\text{O}$  nanofluid.

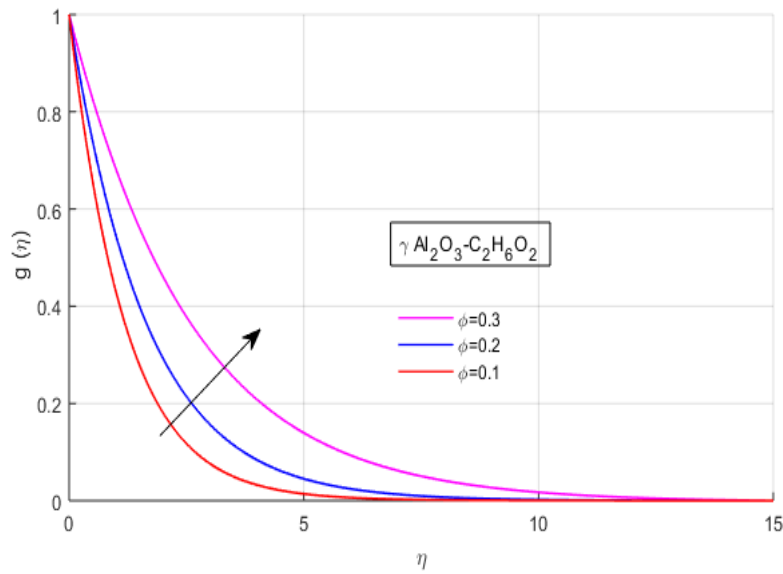
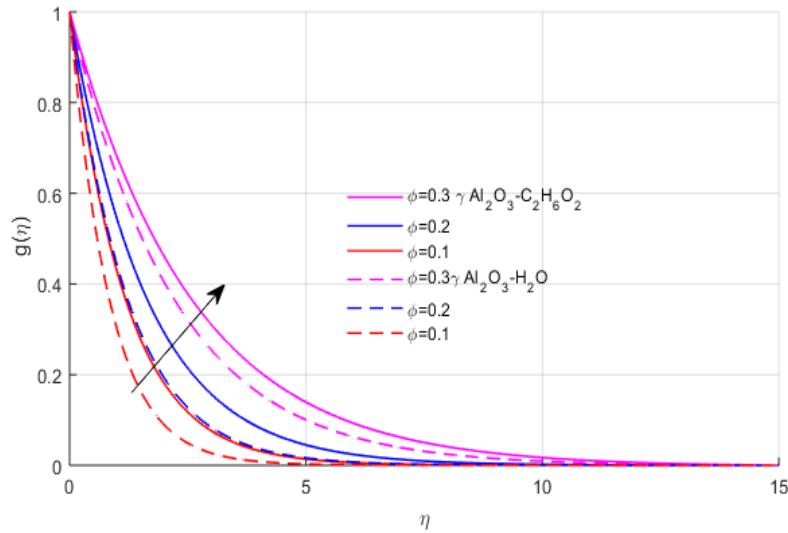


Figure 3.6: Variation in  $g(\eta)$  versus  $\phi$ , when  $Pr = 6.4, B_i = 8.5, C = 1$ , for the  $\gamma\text{Al}_2\text{O}_3 - \text{C}_2\text{H}_6\text{O}_2$ .



**Figure3.7:** Variation in  $g(\eta)$  versus  $\phi$ , when  $Pr = 6.4, B_i = 8.5, C = 1$ , for the nanofluids  $\gamma Al_2O_3 - H_2O$  and  $\gamma Al_2O_3 - C_2H_6O_2$ .

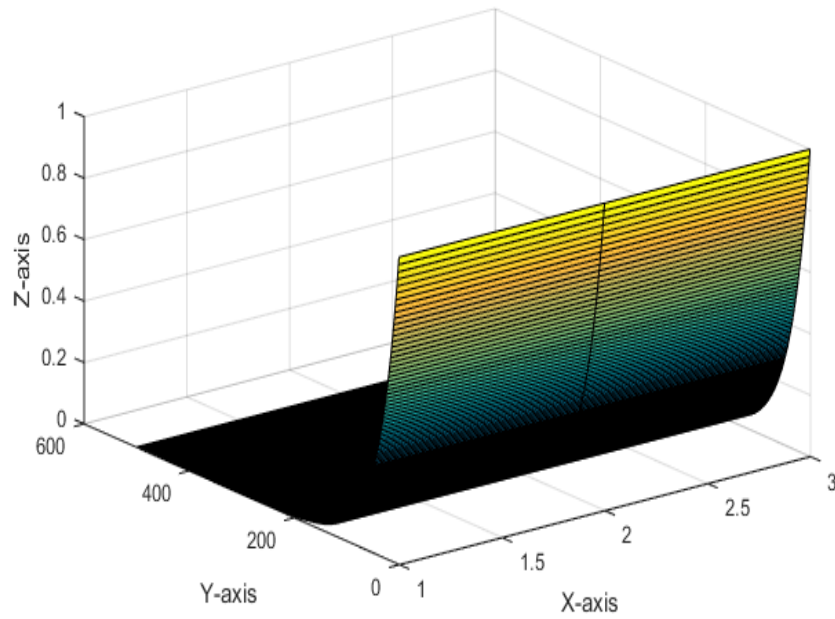


Figure 3.8: Variation in  $g(\eta)$  with the deviation in  $\phi$ , when  $Pr = 6.4, B_i = 8.5, C = 1$ , 3D presentation

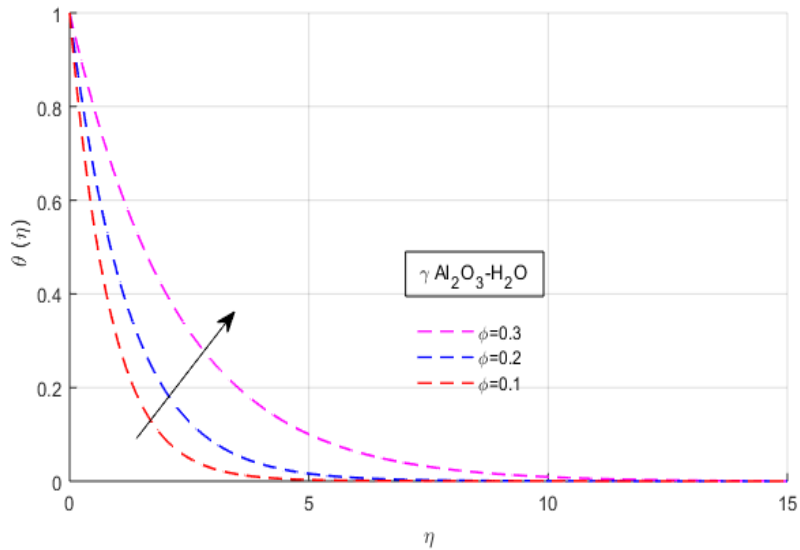
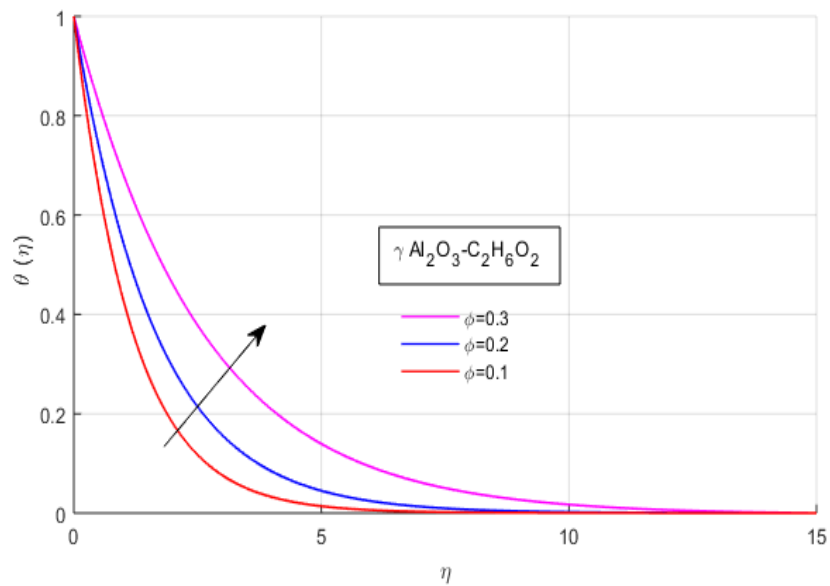
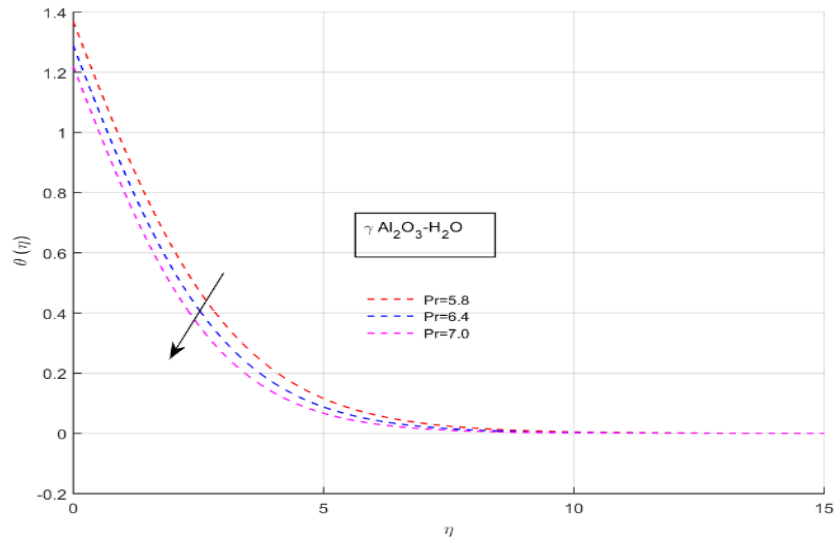


Figure 3.9: Variation in  $\Theta(\eta)$  versus  $\phi$ , when  $Pr = 6.4, B_i = 8.5, C = 1$ , for the  $\gamma Al_2O_3 - H_2O$  nanofluids.





**Fig. 3.10:** Variation in  $\Theta(\eta)$  versus  $\phi$ , when  $Pr = 6.4, B_i = 8.5, C = 1$ , for the nanofluids  $\gamma Al_2O_3 - C_2H_6O_2$ .



**Figure 3.11:** Variation in  $\Theta(\eta)$  versus  $Pr$ , when  $\phi = 0.1, B_i = 8.5, C = 1$ , for the nanofluids  $\gamma Al_2O_3 - H_2O$ .

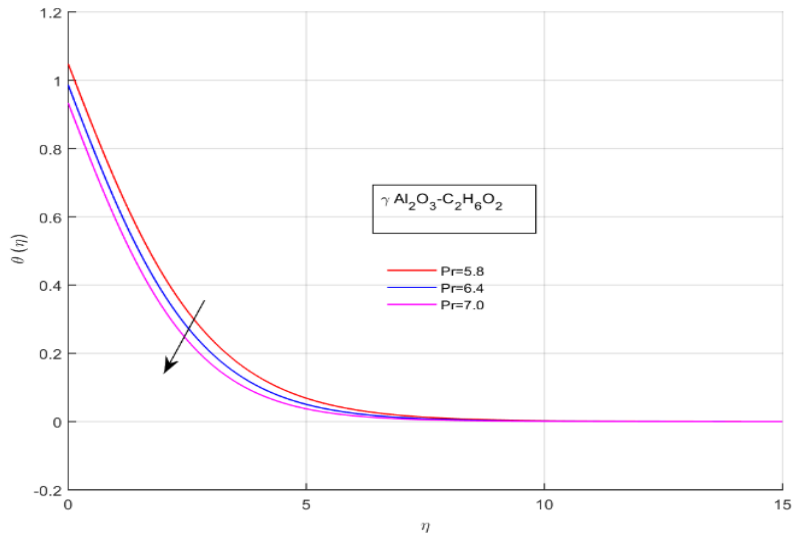


**Fig. 3.12:** Variation in  $\Theta(\eta)$  versus  $Pr$ , when  $\phi = 0.1, B_i = 8.5, C = 1$ , for the nanofluid  $\gamma Al_2O_3 - C_2H_6O_2$ .

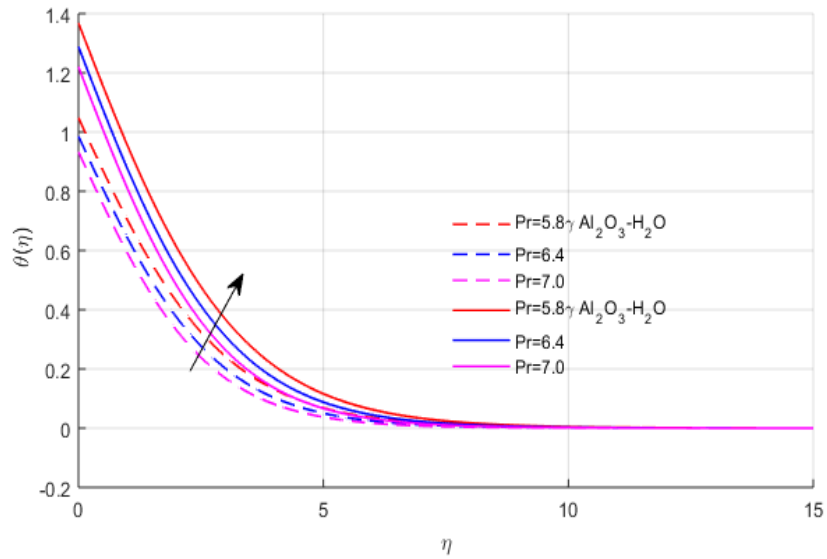


Figure 3.13:  $\Theta(\eta)$  versus  $Pr$ , when  $\phi = 0.1, B_i = 8.5, C = 1$ , for  $O$  and  $\gamma Al_2O_3 - H_2O$  and  $\gamma Al_2O_3 - C_2H_6O_2$ .

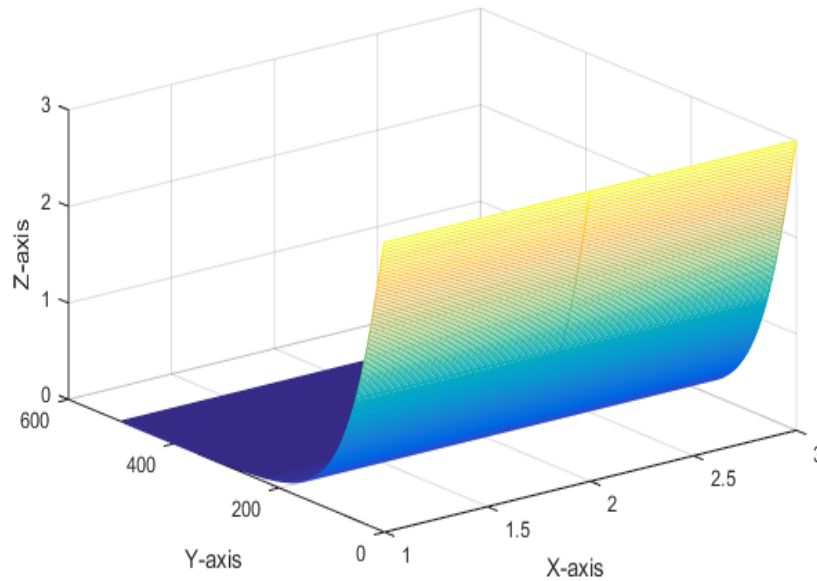


Figure 3.14: Variation in  $\Theta(\eta)$  with the deviation in  $Pr$ , when  $\phi = 0.1, B_i = 8.5, C = 1$ , 3D representation.

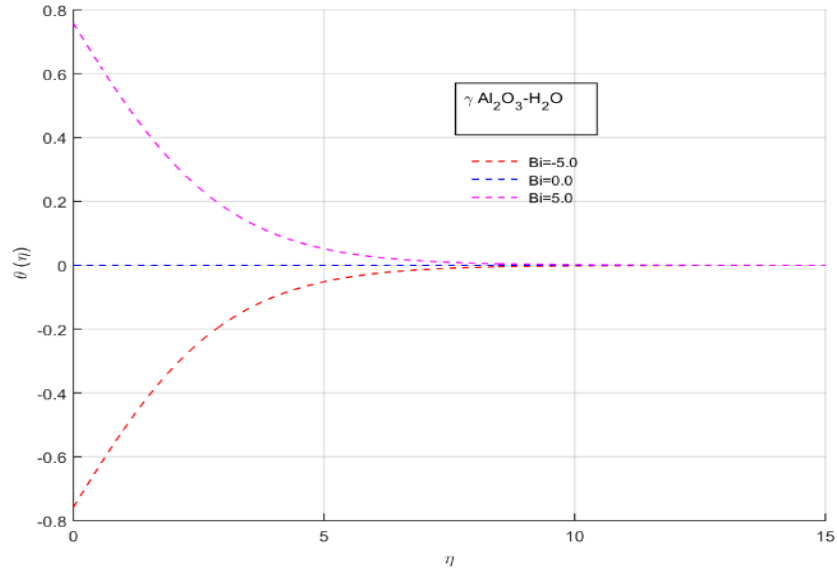


Figure 3.15: Variation in  $\Theta(\eta)$  versus  $B_i$ , when  $\phi = 0.1$ ,  $\text{Pr} = 6.4$ ,  $C = 1$ , for the Nano-fluids  $\gamma\text{Al}_2\text{O}_3 - \text{H}_2\text{O}$ .

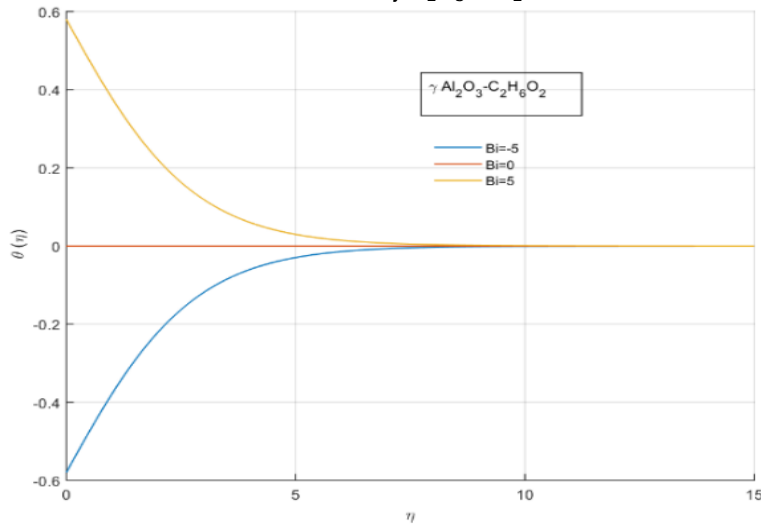


Figure 3.16: Variation in  $\Theta(\eta)$  versus  $B_i$ , when  $\phi = 0.1$ ,  $\text{Pr} = 6.4$ ,  $C = 1$ , for the nanofluids  $\gamma\text{Al}_2\text{O}_3 - \text{C}_2\text{H}_6\text{O}_2$ .

## Results & Discussion

This segment explored the behavior of temperature and velocity distributions under the impact of embedded parameters. The important features of the study in the form of Nusselt number (heat transfer rate)  $Nu$  and skin friction (drag force at the surface)  $C_f$  have been calculated for the  $\gamma Al_2O_3 - C_2H_6O_2$  and  $\gamma Al_2O_3 - H_2O$  Nano fluids. The Biot number  $Bi$  shows the important applications for the thermal/cooling enhancements. The effects of various physical parameters have been displayed in Figs [3.2-3.17].

The physical assembly of the problem is displayed in Fig.1. The nanoparticle volume fraction  $\phi$  effect of the nanoparticle for the  $\gamma Al_2O_3 - H_2O$  nanofluid is shown in Fig. 3.2. The radial velocity  $\frac{df(n)}{dn}$  for the  $Bi > 0$  increases when the increment in the  $\phi$  increases. In fact, the Alumina or other metal nanoparticles are usually used in fluids for increases the heat transfer applications. Because of these reasons, the viscous forces are becoming feeble to stop the fluid motion. Therefore, the larger amount of the nanoparticle volume fraction  $\phi$  raises the velocity field.

The combined effect of the  $\phi$  on the Nano-fluids  $\gamma Al_2O_3 - H_2O$  and  $\gamma Al_2O_3 - C_2H_6O_2$  is shown in Fig.3.4. This is clear that the absorption of the alumina nanoparticles in ethylene glycol generates more energy as compared to the alumina absorption in water. The 3D representation has also authenticated the radial flow pattern as displayed in Fig.3.5. Fig. 3.6 presents that how the greater quantity of the nanoparticle volume fraction  $\phi$  affects the azimuthal velocity  $g(\eta)$ . It has been detected that velocity  $g(\eta)$  is increasing as the  $\phi$  rising for the  $\gamma Al_2O_3 - C_2H_6O_2$  nanofluids. Due to the large amount of  $\phi$ , the tendency of the viscous forces going down and the fluid motion improves. Also, this effect is more efficient  $\gamma Al_2O_3 - C_2H_6O_2$  nanofluids as shown in Fig.3.7.

The combined effect of the  $\gamma Al_2O_3 - H_2O$  and  $\gamma Al_2O_3 - C_2H_6O_2$  nanofluids has been shown in Fig.3.8. It is observed that the fluid motion is more efficient using the  $\gamma Al_2O_3 - C_2H_6O_2$  nanofluid, because as compared to the use of  $\gamma Al_2O_3 - H_2O$  the cohesive forces are more affected between the fluid molecules. 3D representation of the azimuthal velocity  $g(\eta)$  is shown in Fig.3.9. The influence of the nanoparticles of volume fraction  $\phi$  on the temperature field is displayed in Fig.3.10.

The nanoparticles of metals are usually used for thermal enhancement. So the larger amount of  $\phi$  enhance the temperature field for the positive values of  $Bi$ . This effect is similar to  $\gamma Al_2O_3 - H_2O$  and  $\gamma Al_2O_3 - C_2H_6O_2$  nanofluids displayed in Figs. 3.10, 3.11. Fig. 3.12 shows the influence of the Prandtl number on the temperature field. Apparently, with the help of the figure, it is confirmed that the greater extent of  $Pr$  (Prandtl number) temperature pitch  $\Theta(\eta)$  of  $\gamma Al_2O_3 - C_2H_6O_2$   $\gamma Al_2O_3 - H_2O$  nano-liquids is exhibiting decelerating behavior. Mainly  $Pr$  is explained as the ratio of momentum diffusivity to thermal diffusivity. As a result, the larger rate of the  $Pr$  increase the boundary film thickness, which enriches the nanoparticles' cooling effect.

The comparison of the nanofluids  $\gamma Al_2O_3 - C_2H_6O_2$  and  $\gamma Al_2O_3 - H_2O$  for the same values of  $\phi$  is shown in Figs. 3.13, 3.14. It is observed that the mixing of alumina in ethylene glycol is better than the mixing of alumina in water for the heat transfer enhancement and as well for the cooling applications. The 3D configuration for the temperature field is also displayed in the same Fig.3.15. The 3D presentation of the temperature field authenticates the thermal boundary layer path. Figs. 3.16 3.17 portray the behavior of thermal fields  $\Theta(\eta)$  for  $Bi$ . Three different categories ( $Bi > 0, Bi = 0, Bi < 0$ ) for the Biot number have been displayed. The positive value  $Bi > 0$  shows the enhancement in the temperature field. The zero value  $Bi = 0$  means no thermal convection exists and the  $Bi < 0$  shows reverse effect. The figures 3.16, 3.17 show that this impact is comparatively rapid in  $\gamma Al_2O_3 - C_2H_6O_2$ .

Table 1 shows the physical characteristics such as ( $Pr, Cp, K, \rho$ ) of  $\gamma Al_2O_3, H_2O, C_2H_6O_2$ . In Table 2, the external drag force rising for the larger extent of nanoparticles, the greater amount of  $\phi$  increasing the thickness to improve the resistance force and as a result, it increases the skin friction. Whereas the heat transfers ( $Nu$ ) declined. The same effect has been observed for the  $\gamma Al_2O_3 - C_2H_6O_2$  nanofluid in Table 3. From the above two tables it has been detected that  $\gamma Al_2O_3 - C_2H_6O_2$  nanofluid is more efficient than the  $\gamma Al_2O_3 - H_2O$  nanofluid for enhancement and cooling effects.

### Conclusion

In this analysis, we investigated the three-dimensional flow of  $\gamma Al_2O_3 - H_2O$  and  $\gamma Al_2O_3 - C_2H_6O_2$  nanofluids on the rotating disk.

The convective thermal conditions play an important role to enhance the temperature field rapidly. The numerical RK4 has been applied to the flow problems. The main outcome of this analysis is to increasing values of the nanoparticle causes a decreasing velocity field and this is a more effective decline for  $\gamma Al_2O_3 - C_2H_6O_2$  nano-liquid.

All through the outcomes, we foresee that temperature pitch quickly enhanced for nanofluid For  $\gamma Al_2O_3 - C_2H_6O_2$  nanofluid as related to nanofluids  $\gamma Al_2O_3 - H_2O$ . The main characters of the flow problem grow the huge quantity of the nanoparticles. For  $\gamma Al_2O_3 - H_2O$  Nusselt number (heat transfer rate) is stronger versus  $\gamma Al_2O_3 - C_2H_6O_2$  nanofluid. From the present analysis we also noticed that the maximum amount of Prandtl number  $Pr$ , minimizing the temperature and more powerful by discussing that kind of  $\gamma Al_2O_3 - C_2H_6O_2$  nanofluid. Surely mentioned sorts of nanofluid that is  $\gamma Al_2O_3 - C_2H_6O_2$  and  $\gamma Al_2O_3 - H_2O$  must be utilized in numerous manufacturing purposes, Refrigeration/heating agents, coating processes, thermal and coating idea and many more purposes.

### Declarations

It is to declare that the authors have no funding and conflict of interests. The authors declare that they have no competing interests.

### Acknowledgment

I would like to express my deep gratitude to Dr. Amanat Ali Shah for his valuable and constructive suggestions during the planning and development of this research work. His willingness to give so generously of his time was greatly appreciated. I would also like to thank Dr. Jamal Uddin for his advice and help in keeping my progress on schedule. I am also thankful to Mr. Muhammad Asim Ullah for helping me in developing the research methodology and Mr. Izaz Ali who helped me to complete this research work. Finally, I would like to thank my parents for their support and encouragement during my studies.

### References

- Ahmed, N., Adnan, Khan, U., & Mohyud-Din, S. T. (2017). Influence of an effective Prandtl number model on squeezed flow of  $\gamma Al_2O_3 - H_2O$  and  $\gamma Al_2O_3 - C_2H_6O_2$  nanofluids. *Journal of Molecular Liquids*, 238, 447–454.
- The Sciencetech* 138 Volume 4, Issue 2, April-June 2023

- <https://doi.org/10.1016/j.molliq.2017.05.049>
- Ahmed, N., Adnan, Khan, U., & Mohyud-Din, S. T. (2018). A theoretical investigation of unsteady thermally stratified flow of  $\gamma\text{Al}_2\text{O}_3\text{-H}_2\text{O}$  and  $\gamma\text{Al}_2\text{O}_3\text{-C}_2\text{H}_6\text{O}_2$  nanofluids through a thin slit. *Journal of Physics and Chemistry of Solids*, 119, 296–308. <https://doi.org/10.1016/j.jpcs.2018.01.046>
- Alshomrani, A. S., & Gul, T. (2017). A convective study of  $\text{Al}_2\text{O}_3\text{-H}_2\text{O}$  and  $\text{Cu-H}_2\text{O}$  nano-liquid films sprayed over a stretching cylinder with viscous dissipation. *European Physical Journal Plus*, 132(11). <https://doi.org/10.1140/epjp/i2017-11740-1>
- GANDI, C. J. (2016). *EXPERIMENTAL AND NUMERICAL STUDY OF HEAT TRANSFER PHENOMENON IN A MICRO DROPLET REACTOR*. 147(March), 11–40.
- Gul, T., Afridi, S., Ali, F., Khan, I., & Alshomrani, A. S. (2018). Heat transmission in the liquid film flow of micropolar fluid in a porous medium over a stretching sheet with thermal radiation. *Journal of Nanofluids*, 7(2), 316–324. <https://doi.org/10.1166/jon.2018.1447>
- Hatami, M., Sheikholeslami, M., & Ganji, D. D. (2014). Laminar flow and heat transfer of nanofluid between contracting and rotating disks by least square method. *Powder Technology*, 253, 769–779. <https://doi.org/10.1016/j.powtec.2013.12.053>
- Khan, N. S., Gul, T., Islam, S., Khan, A., & Shah, Z. (2017). Brownian motion and thermophoresis effects on MHD mixed convective thin film second-grade nanofluid flow with hall effect and heat transfer past a stretching sheet. *Journal of Nanofluids*, 6(5), 812–829. <https://doi.org/10.1166/jon.2017.1383>
- Khan, U., Adnan, Ahmed, N., & Mohyud-Din, S. T. (2017). 3D squeezed flow of  $\gamma\text{Al}_2\text{O}_3\text{-H}_2\text{O}$  and  $\gamma\text{Al}_2\text{O}_3\text{-C}_2\text{H}_6\text{O}_2$  nanofluids: A numerical study. *International Journal of Hydrogen Energy*, 42(39), 24620–24633. <https://doi.org/10.1016/j.ijhydene.2017.07.090>
- Khan, W., Gul, T., Idrees, M., Islam, S., & Khan, I. (2017). Dufour and Soret effect with thermal radiation on the nanofilm flow of Williamson fluid past over an unsteady stretching sheet. *Journal of Nanofluids*, 6(2), 243–253. <https://doi.org/10.1166/jon.2017.1328>
- Kulkarni, D. P., Vajjha, R. S., Das, D. K., & Oliva, D. (2008). Application of aluminum oxide nanofluids in diesel electric generator as jacket water coolant. *Applied Thermal Engineering*, 28(14–15), 1774–1781. <https://doi.org/10.1016/j.applthermaleng.2007.11.017>

- Maciver, D. S., Tobin, H. H., & Barth, R. T. (1963). Catalytic aluminas I. Surface chemistry of eta and gamma alumina. *Journal of Catalysis*, 2(6), 485–497. [https://doi.org/10.1016/0021-9517\(63\)90004-6](https://doi.org/10.1016/0021-9517(63)90004-6)
- Mahadevappa, P. (1980). A Study on the Behaviour of Steel. *Building and Environment*, 15(5), 191–195.
- Maré, T., Sow, O., Halefadl, S., Lebourlout, S., & Nguyen, C. T. (2012). Experimental study of the freezing point of  $\gamma$ -Al<sub>2</sub>O<sub>3</sub>/water nanofluid. *Advances in Mechanical Engineering*, 2012. <https://doi.org/10.1155/2012/162961>
- Moatimid, G. M., Hassan, M. A., & Mohamed, M. A. A. (2020). Temporal instability of a confined nano-liquid film with the Marangoni convection effect: viscous potential theory. *Microsystem Technologies*, 26(6), 2123–2136. <https://doi.org/10.1007/s00542-020-04772-2>
- Mukhopadhyay, S., & Nimbalkar, G. (2021). Fundamental study on chaotic transition of two-phase flow regime and free surface instability in gas deaeration process. *Experimental and Computational Multiphase Flow*, 3(4), 258–288. <https://doi.org/10.1007/s42757-020-0065-3>
- Nguyen, C. T., Roy, G., Gauthier, C., & Galanis, N. (2007). Heat transfer enhancement using Al<sub>2</sub>O<sub>3</sub>-water nanofluid for an electronic liquid cooling system. *Applied Thermal Engineering*, 27(8–9), 1501–1506. <https://doi.org/10.1016/j.applthermaleng.2006.09.028>
- Rashidi, M. M., Kavyani, N., & Abelman, S. (2014). International Journal of Heat and Mass Transfer Investigation of entropy generation in MHD and slip flow over a rotating porous disk with variable properties. *International Journal of Heat and Mass Transfer*, 70, 892–917. <https://doi.org/10.1016/j.ijheatmasstransfer.2013.11.058>
- Rashidi, M. M., Vishnu Ganesh, N., Abdul Hakeem, A. K., Ganga, B., & Lorenzini, G. (2016). Influences of an effective Prandtl number model on nano boundary layer flow of  $\gamma$  Al<sub>2</sub>O<sub>3</sub>-H<sub>2</sub>O and  $\gamma$  Al<sub>2</sub>O<sub>3</sub>-C<sub>2</sub>H<sub>6</sub>O<sub>2</sub> over a vertical stretching sheet. *International Journal of Heat and Mass Transfer*, 98, 616–623. <https://doi.org/10.1016/j.ijheatmasstransfer.2016.03.006>
- Sebdani, S. M., Mahmoodi, M., & Hashemi, S. M. (2012). Effect of nanofluid variable properties on mixed convection in a square cavity. *International Journal of Thermal Sciences*, 52(1), 112–126. <https://doi.org/10.1016/j.ijthermalsci.2011.09.003>
- Sheikholeslami, M., Hatami, M., & Ganji, D. D. (2015). Numerical



- investigation of nano fluid spraying on an inclined rotating disk for cooling process. *Journal of Molecular Liquids*, 211, 577–583. <https://doi.org/10.1016/j.molliq.2015.07.006>
- Tahir, F., Gul, T., Islam, S., Shah, Z., Khan, A., Khan, W., ... Muradullah. (2017). Flow of a nano-liquid film of Maxwell fluid with thermal radiation and magneto hydrodynamic properties on an unstable stretching sheet. *Journal of Nanofluids*, 6(6), 1021–1030. <https://doi.org/10.1166/jon.2017.1400>
- Thomas, J. C., & Casasayas, C. O. (2022). *Masters in Energy Engineering Analysis of CO2 Power Cycle Heat Exchangers Escola Tècnica Superior d' Enginyeria Industrial de Barcelona*. (April).
- Turkyilmazoglu, M., & Senel, P. (2013). International Journal of Thermal Sciences Heat and mass transfer of the flow due to a rotating rough and porous disk. *International Journal of Thermal Sciences*, 63, 146–158. <https://doi.org/10.1016/j.ijthermalsci.2012.07.013>
- Turkyilmazoglu, Mustafa. (2014). Computers & Fluids Nanofluid flow and heat transfer due to a rotating disk. *COMPUTERS AND FLUIDS*, 94, 139–146. <https://doi.org/10.1016/j.compfluid.2014.02.009>
- Turkyilmazoglu, Mustafa. (2016). Flow and heat simultaneously induced by two stretchable rotating disks. *American Institute of Physics*, 043601. <https://doi.org/10.1063/1.4945651>
- Umar, K., Adnan, A., Naveed, A., & Tauseef, M. uddin S. (2012). *Engineering Computations*. 6(4), 5–6. <https://doi.org/http://dx.doi.org/10.1108/eb023774>
- Zamzamian, A., Oskouie, S. N., Doosthoseini, A., Joneidi, A., & Pazouki, M. (2011). Experimental investigation of forced convective heat transfer coefficient in nanofluids of Al<sub>2</sub>O<sub>3</sub>/EG and CuO/EG in a double pipe and plate heat exchangers under turbulent flow. *Experimental Thermal and Fluid Science*, 35(3), 495–502. <https://doi.org/10.1016/j.expthermflusci.2010.11.013>